SHEAR STRENGTH AND SNOWPACK STABILITY TRENDS IN NON-PERSISTANT WEAK LAYERS

Catherine Brown[1]* and Bruce Jamieson[1,2]
[1]Dept. of Geoscience, University of Calgary
[2]Dept. of Civil Engineering, University of Calgary

ABSTRACT: Non-persistent weak layers in storm snow exhibit rapidly changing physical and mechanical properties. The shear strength and its rate of change, relevant to storm snow slab avalanches and rarely measured. To measure the shear strength we performed up to 10 sets of 12 shear frame tests for 16 separate storm snow weak layers. Layers were sampled once or twice a day resulting in over 1100 shear frame tests at the Mt. Fidelity, Rogers Pass and Blue River study plots during the winters of 2006 and 2007 in the Columbia Mountains of British Columbia, Canada. Snowpack properties, including overlying load, densities, temperature gradient and crystal types, of the weak layer and adjacent layers were measured, along with atmospheric conditions. We present an empirical strength change model, based on the properties with the greatest influence on strength changes in the weak layers. The model predicts shear strength on a given day, based on standard field measurements, and forecasts the strength of the layer. We compare our measured and modeled strength with output from SNOSS.

KEYWORDS: shear strength, snow stability, avalanche forecasting, non-persistent weak layers

1. INTRODUCTION

There are numerous non-persistent, or storm snow weak layers in alpine snowpacks throughout the winter. These layers can be the failure plane for natural avalanches, which tend to be of concern for avalanche forecasters protecting infrastructure, such as transportations corridors and communities. Storm snow weak layers exhibit rapidly changing structural characteristics after deposition (Brown and Jamieson, 2006), which can result in a weak layer being a concern to forecasters for a short time period. This is compared to persistent weak layers of depth hoar and surface hoar crystals, which can produce numerous avalanche cycles over longer periods.

Shear strength of the weak layer, combined with overburden stress to calculate a stability index is one piece of information about the snowpack that can help predict when natural slab avalanching will occur (e.g. Schweizer and Föhn, 1996). Two stability indices, Sn_{38} (Jamieson and Johnston, 1993; Jamieson, 1995) and SF, 'stability factor' or Stability Ratio (Schleiss and Schleiss, 1970) have been shown useful for forecasting natural avalanche activity. Shear strength is commonly measured using a shear frame test, which requires an experienced observer to perform the test at a site that is representative of the surrounding terrain. Having a method of estimating and forecasting shear strength could be advantageous for daily natural avalanche forecasting.

The goal of this study is to construct a model that relates the strength of non-persistent weak layers with standard observations of snowpack factors. Standard observations may be used to estimate shear strength of identified storm snow weak layers in the Columbia Mountains. The estimate of shear strength can then be used to calculate a stability index for natural avalanches in the Columbia Mountains.

2. METHODS

During the winters of 2006 and 2007 snowpack and weather observations were performed at three study areas in the Columbia Mountains of British Columbia, Canada. The Mt. St. Anne study plot is located in the Mike Wiegele Helicopter Skiing tenure and the Mt. Fidelity and Rogers Pass study plots are located in Glacier National Park (Fig. 1). The Mt. St. Anne study plot has an elevation of 1900 m a.s.l., with a slope angle of 0° and an east aspect. The Mt. Fidelity study plot at the west boundary of Glacier National Park has an elevation of 1905 m a.s.l., with a slope angle of 0° and an east aspect. The Rogers Pass study plot, located adjacent to the Trans-Canada highway, has an elevation of 1315 m a.s.l., with a slope angle of 0°. All three study plots are used by their corresponding operations as sites to obtain daily standard manual and/or automatic snowpack and weather observations.

* *Corresponding author address:* Catherine Brown, Dept. of Geoscience, University of Calgary, 2500 University Dr. NW, Calgary, AB, CANADA T2N 1N4; email: cibrown@ucalgary.ca

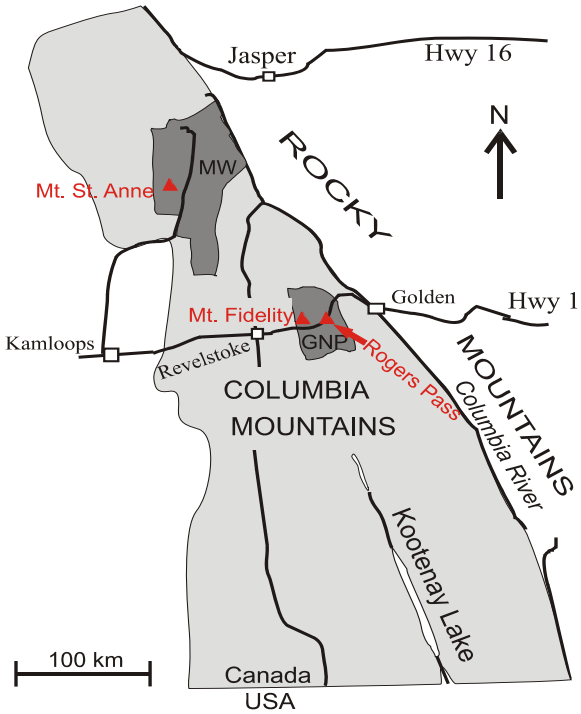

Figure 1. Study area location map of the Columbia Mountains. Mt. Fidelity and Rogers Pass study plots in Glacier National Park (GNP), and Mt. St. Anne study plot in Mike Wiegele Helicopter Skiing tenure (MW).

With the two treeline study plots, Mt. St. Anne and Mt. Fidelity located in sites where observations obtained there can be extrapolated to the surrounding avalanche paths, to give a representative picture of snowpack properties.

At the start of each measurement interval storm snow weak layers were identified using a tilt-board test. The tilt-board test, developed and used for over 40 years in the avalanche forecasting program at Rogers Pass in Glacier National Park (Schleiss and Schleiss, 1970), induces a slope of ~ 15° on an isolated column (0.3 m x 0.3 m, with a height of up to 0.4 m) of storm snow (Green et al., 2004; CAA, 2007). A dynamic load is then applied by an upward manual hit to produce a fracture along a weak layer or failure plane. The tilt-board test also displays the interaction between the slab and weak layer in the upper section of the snowpack, where descriptors of the result of the test such as a 'fast and clean' shear gives the observer information of the characteristic of both the weak layer and slab.

The average shear strength of the weak layer was measured using a shear frame test. We did on average 12 tests in order to obtain a representative strength value across the snow pit wall. The overlying snow was removed, leaving enough to place the shear frame (100 or 250 cm^2) parallel to the weak layer and a few millimeters above it (Sommerfeld, 1984). Further details of the shear frame test method can be found in Jamieson and Johnston (2001). The shear strength is calculated by dividing the maximum reading from the force gauge by the shear frame area and adjusting for size effects (Sommerfeld, 1980; Föhn, 1987). We assume the weak layer is only failing in shear, in order to obtain a measure of shear strength.

Overlying load (vertical weight per unit area) of the slab was the average value from vertical core samples from snow surface to the weak layer (Jamieson and Johnston, 1999). The load, σ, is calculated using Eq. (1),

$$\sigma = \rho g H \qquad (1)$$

where, ρ is the average density of the overlying slab, g is the acceleration due to gravity, and H is the thickness of the slab measured vertically.

At each measurement interval, we completed a standard snow profile consistent with observation guidelines (CAA, 2007) to a depth of one layer below the weak layer of interest. Two compression tests with fracture character observations were performed with each profile (CAA, 2007). Manual temperatures of the weak layer, 5 cm above and below the weak layer were measured to obtain the temperature gradient across the failure plane. Density measurements for layers with a thickness of ≥ 1 cm were obtained using custom-built samplers. We measured weak layer thickness to the nearest millimeter.

3. OBSERVATIONS

We initiated measurements of the weak layer, snowpack and weather conditions as soon after the weak layer was buried as possible. In the first few days of sampling when weak layer conditions were changing rapidly, observations were made twice daily in order to accurately measure the evolution in shear strength. After the initial strengthening period, we proceeded with daily measurements until the layer was no longer identifiable on the snow pit wall, which often coincided with the weak layer not reacting in the tilt-board test, or 8 days after deposition.

Over 1100 shear strength measurements from 95 measurement intervals and 16 separate weak layers were used to construct and test the strength change model (Table 1) Weak layers

Table 1. Storm snow layers measured and used for model construction and model testing (highlighted).

Weak Layer Date	Location	N
8-Jan-06	Mt. Fidelity Study Plot	3
10-Jan-06	Mt. Fidelity Study Plot	2
16-Jan-06	Mt. Fidelity Study Plot	9
19-Jan-06	Mt. Fidelity Study Plot	2
22-Jan-06	**Mt. Fidelity Study Plot**	**5**
1-Feb-06	Mt. Fidelity Study Plot	8
21-Feb-06	Mt. Fidelity Study Plot	7
7-Jan-07	Rogers Pass Study Plot	5
16-Jan-07	Mt. Fidelity Study Plot	10
18-Jan-07	Mt. Fidelity Study Plot	6
23-Jan-07	Mt. St. Anne Study Plot	5
5-Feb-07	Mt. Fidelity Study Plot	9
9-Feb-07	Mt. St. Anne Study Plot	5
12-Feb-07	**Mt. Fidelity Study Plot**	**6**
18-Feb-07	Mt. Fidelity Study Plot	9
3-Mar-07	Mt. St. Anne Study Plot	4
	Total Measurement Intervals	95

were observed between 2 and 10 times. Figure 2 shows an example of a typical time series of shear strength and load measurements on a storm snow weak layer deposited on January 16, 2006.

Storm snow weak layers had lower densities and larger crystals with higher dendricity when compared to layers above and below (Figure 3). A more complete report of weak layer characteristics is found in Brown and Jamieson (2006).

4. RESULTS

4.1 Model building

We formulated a simple empirical strength change model to: (A) estimate weak layer shear strength on the day snowpack observations are made and, (B) forecast the shear strength for up to 8 days after the initial measurement interval.

This analysis uses the same equation used by Chalmers (2001) in his interval model to forecast shear strength in surface hoar layers, and later refined by Zeidler (2004) for other persistent instabilities,

$$\Sigma_j^* = \Sigma_i^* + \Delta t_{ij}(\Delta\Sigma/\Delta t)_{ij}^* \qquad (2)$$

Σ_i^* is the estimated shear strength on day i (kPa), Δt_{ij} is the time interval between day i and day j (t_j - t_i), $(\Delta\Sigma/\Delta t)_{ij}^*$ is the estimated rate of change in shear strength (kPa d^{-1}) between day i and day j, and Σ_j^* is the forecasted shear strength of day j (kPa). We seek simple models for estimating the

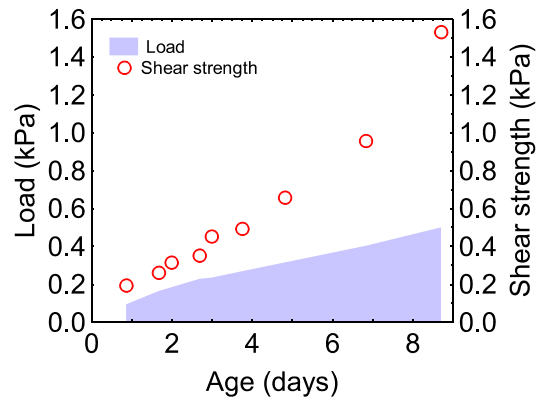

Figure 2. Time series of shear strength and load measurements from a weak layer deposited on 16-Jan-06.

shear strength on a day with manual observations Σ_i^*, and the rate of change since the last observation day $(\Delta\Sigma/\Delta t)_{ij}^*$.

In order for the model to be operational useful, only easily measurable predictor variables were chosen (Table 2). Also, only those that showed a significant correlation with Σ_i^* or $(\Delta\Sigma/\Delta t)_{ij}^*$ based on a Spearman rank correlation were included as input variables in the respective models.

None of the possible predictor variables measured had strong enough correlations with the shear strength change term, $(\Delta\Sigma/\Delta t)_{ij}^*$ to be selected as input variables. The predictor variables, load, temperature gradient across the weak layer, temperature 5 cm above the weak layer, slab thickness, weak layer temperature, minimum snow crystal size, and initial shear strength, all had a p-level < 0.05 in Spearman rank correlations, but the highest Spearman r = 0.363 for load. In this study possible predictors were only chosen if r ≥ 0.8.

To estimate shear strength Σ_i^*, we used a backwards stepwise multiple regression (Wilks, 1995). Prior to regression, correlation analysis between the possible predictor variables was performed. Variables with high cross-correlation (r > 0.8) resulted in exclusion of one of the variables if it did not add physically relevant information to the regression. The multiple regression analysis was validated by residual analysis. Since the hypothesis of normality for the shear strength distribution is rejected, we tried a logarithmic transformation of Σ_i^*, which resulted in a normal distribution of measured shear strength.

The results of this regression are shown in Table 3 for ln Σ_i^*.

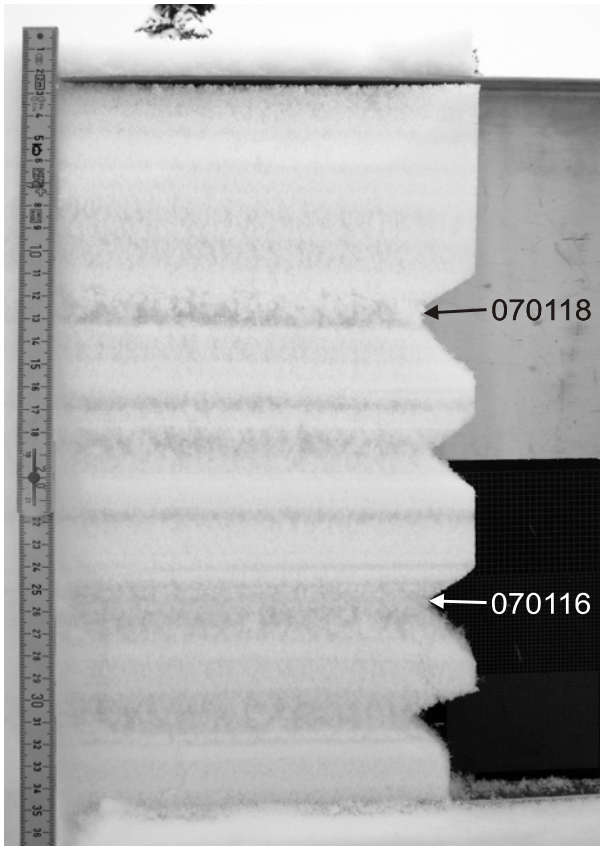

Figure 3. In-situ picture taken on 19-Jan-07 of the top 35 cm of snow in the Mt. Fidelity study plot. Arrows point to where the failure occurred in two measured weak layers deposited on 16-Jan-07 and 18-Jan-07. Weak layer 16-Jan-07 had a ρ = 42 kg m^{-3}, thickness of 25 mm, and consisted of stellar crystals, size 1-2 mm. Weak layer 18-Jan-07 had a ρ = 50 kg m^{-3}, thickness of 15 mm, and consisted of stellar crystals, size 3-6 mm.

The regression results derived the empirical formula for Σ_i* (kPa):

$$\Sigma_i^* = e \wedge (0.211 \bullet \text{Age (day)} + 0.0204 \bullet \text{H (m)} + 0.00636 \bullet \text{Slabdens (kg m}^{-3}) - 0.00661 \bullet \text{T-5}^2\,(°\text{C}) - 2.80). \quad (3)$$

Slab density (Slabdens) can be expressed in terms of H and Load, which are easy to measure

$$\text{Slabdens} = \text{Load} / gH \quad (4)$$

Table 2. Predictor variables and units for response variable, Σ_i.*

Variable	Description (units)
Age	Age of the weak layer (days); number of days since buried
E_{min}	Minimum grain size of weak layer crystal (mm)
E_{max}	Maximum grain size of weak layer crystal (mm)
Load	Vertical load (force per unit area) of snow overlying the weak layer (kPa)
H	Thickness of snow slab overlying the weak layer (m)
Thick	Thickness of the weak layer (cm)
Density	Density of the weak layer (kg m^{-3})
T_{-5}	Temperature 5 cm below the weak layer (°C)
TG	Magnitude of temperatue gradient across weak layer(°C m^{-1})
Slabdens	Density of the snow slab overlying the weak layer (kg m^{-3})

where, Load is the weight per unit area of the slab vertically overlying the weak layer, g is the

acceleration due to gravity, and H is the depth of the weak layer.

Rewriting Eq. 3 and Eq. 4 yields:

$$\Sigma_i^* = e \wedge (0.211 \bullet \text{Age (day)} + 0.0204 \bullet \text{H (m)} + 0.00636 \bullet (\text{Load} / gH) - 0.00661 \bullet \text{T-5}^2\,(°\text{C}) - 2.80). \quad (5)$$

In order understand the relationship between each independent significant predictor variable and initial shear strength a discussion of each follows. Similar to Zeidler (2004), the evaluation is based mainly on the sign of the coefficients of each predictor variable (Table 3), were a '+' sign indicates a positive relationship and a '-' sign indicates a negative relationship.

4.1.1 Age of the weak layer (Age)

Immediately after deposition fresh, new snow crystals with high dendriticy are metamorphosing rapidly to reduce surface area and bond are formed (Gubler, 1982; Colbeck, 1997; Brown et al., 2001) causing the layer to gain strength. Bond growth rate then decays as bonds and crystals move closer to an equilibrium shape.

Table 3. Multiple backwards stepwise regression on ln Σ_i*.

N = 77	B	Standard Error B	Significance Level *p*	Tolerance	Adjusted r^2	Standard Error of Estimate	*p*
Intercept	-2.80	0.193	<1E-17				
Age	0.211	0.030	6.5E-10	0.67			
H	0.0204	0.003	1.0E-07	0.68	0.80	0.355	1.0E-17
Slabdens	0.00636	0.001	1.7E-05	0.82			
$T\text{-}5^2$	-0.00661	0.001	1.2E-08	0.88			

4.1.2 Thickness of snow slab overlying the weak layer (H)

As the weak layer is buried more deeply, the weight of the overlying snow slab increases. An increase in load causes densification and pressure sintering. Densification reduces the amount of pore space in the ice lattice comprising the weak layer, increasing the contact points and bonds between snow crystals (Kojima, 1967 and Conway and Wilbour, 1999). Pressure sintering can be a dominant process in bond formation between ice grains, where bonds form due to the forces pushing the grains together producing pressure melting at the contact point and subsequent melting and bond formation (Gubler, 1982; Szabo and Schneebeli, 2006). Pressure sintering resulting in an increasing number of bonds per unit area will strengthen the layer.

4.1.3 Density of snow slab overlying the weak layer (Slabdens)

The positive correlation indicates that denser slabs typically overly stronger weak layers. Denser slab are older slabs which are apply more load on the weak layer than younger, lighter slabs. Stronger weak layers exist likely due to the processes of densification and pressure sintering.

4.1.4 Temperature 5 cm below the weak layer ($T\text{-}5^2$)

The negative coefficient multiplied by a temperature (always negative in our data) increases the estimated strength for colder snow. Colder snow temperatures produce stronger snowpack temperature gradients, which can cause increased bond formation between snow crystals due to the greater movement of water molecules (Colbeck, 1997).

The model produced in Eq.5 to estimate initial shear strength was tested for fit to the data used to construct it. Predicted shear strength was computed and compared to measured shear strength. The model test of fit yields an R^2 of 0.82 and a sum of residuals squared of 0.69 (kPa^2). The model explains 82% of the variability in the dataset used to construct the model.

The results of the Spearman rank correlation revealed no significant correlations between measured predictor variables and $(\Delta\Sigma/\Delta t)_{ij}$*. Zeidler (2004) encountered a similar problem when attempting to determine a strength change term for persistent weak layers. She suggested using either a daily loading rate or an average loading rate to determine the amount of strengthening in a weak layer over a given time period. This would be appropriate given the strong correlation between shear strength and load in this study and other studies on persistent weak layers (Johnson, 2001; Chalmers, 2001; Zeidler, 2004).

Using an average loading rate for the Mt. Fidelity study plot of 0.062 kPa d^{-1} (calculated from Schleiss, 1989) the equation for $(\Delta\Sigma/\Delta t)_{ij}$* becomes,

$$(\Delta\Sigma/\Delta t)_{ij}^* = 0.062 \bullet \Delta t_{ij}. \quad (6)$$

Or using a daily loading rate term,

$$(\Delta\Sigma/\Delta t)_{ij}^* = (Pcp_{ij}/\Delta t_{ij})^*\Delta t_{ij} \quad (7)$$

where Pcp_{ij} is the daily load in kPa. The daily load can be measured from adjacent automatic weather stations giving hourly readings of load from an automatic precipitation gauge. Alternatively, from a representative study plot, manual readings of load can be obtained from core tube sampling.

Three different strength change terms were assessed, average, daily automatic, and daily manual. Daily automatic load measurements were only available for measurement intervals at the Mt. Fidelity Study Plot which had an automatic precipitation gauge. Daily manual load

measurements were obtained from core tube loads taken at every measurement interval. When comparing predicted shear strength with measured shear strength in the model building dataset, the daily automatic loading rate has the lowest error (sum of residuals squared) = 0.56 kPa^2, followed by daily manual loading rate and average loading rate, 0.70 kPa^2 and 0.77 kPa^2 respectively. r^2 = 0.88 using the daily automatic loading rate, followed by 0.83 and 0.81, for the daily manual loading rate and average loading rate, respectively.

Based on these results we present two variations of the shear strength forecast model. The first uses the daily manual loading rate (for use when manual core load measurements are available),

$$\Sigma_j^* = e \wedge (0.211 \bullet \text{Age (day)} + 0.0204 \bullet \text{H (m)} + 0.00636 \bullet (\text{Load} / gH) - 0.00661 \bullet T\text{-}5^2 (°C) - 2.80) + (PcpM_{ij}/\Delta t_{ij})*\Delta t_{ij} \quad (8)$$

where $PcpM_{ij}$ is the increase in load between day *i* and day *j* from manual core tube samples taken from a representative study plot.

Alternatively, using automatic load measurements,

$$\Sigma_j^* = e \wedge (0.211 \bullet \text{Age (day)} + 0.020 \bullet \text{H (m)} + 0.006 \bullet (\text{Load} / gH) - 0.007 \bullet T\text{-}5^2 (°C) - 2.80) + PcpA_{ij}\Delta t_{ij} \quad (9)$$

where $PcpA_{ij}$ is the increase in load between day *i* and day *j* obtained from an automatic precipitation gauge. Due to the inaccuracies of using an automatic precipitation gauge to measure snowfall amounts a regression was performed between measured core tubes and recorded snow water equivalent (SWE) for every interval at Mt. Fidelity. The result of this regression in Eq. 10 shows the relationship between automatic and manual load measurements,

$$PcpA_{ij}/\Delta t_{ij} = (0.092 + 0.0045 * PcpG_{ij}/\Delta t_{ij}) \quad (10)$$

where $PcpG_{ij}$ is the change in SWE recorded by the precipitation gauge between day *i* and day *j*.

4.2 Model testing

Two time series of non-persistent weak layers were excluded from model construction (Table 1) in order to test the model. Using both models (Eq 8. + 9.) for these time series, a %error of the measured to forecasted values was obtained of the 'End' shear strength value. Where,

$$\%\text{error} = 100|\Sigma_{measured} - \Sigma_{forecast}|/\Sigma_{measured}. \quad (11)$$

At the end of the time series the model had an average error of 26% and 29%, using daily automatic loading rate and daily manual loading rate respectively.

5. SNOSS

SNOSS is a physically based model (with empirical parameterizations) model developed at the University of Washington that calculates a stability index and estimates a time of failure (avalanche release) in storm snow, that can be run entirely on automatic weather observations (Conway and Abrahamson, 1988; Conway and Wilbour, 1998, 1999; Hayes et al., 2004). SNOSS requires an initial input of air temperature at the time of weak layer deposition (if a manual density measurement is unavailable) to determine weak layer density and calculate shear stress. After deposition hourly measurements of precipitation and temperature are used to calculate components of shear stress and strength. SNOSS produces at stability index each hour and an expected time to failure (avalanche release). In the following analysis we run SNOSS with measurements of snowpack and weather conditions from one time series from Mt. Fidelity. The expected time of failure is compared with avalanche activity observations from the surrounding highway corridor.

The time series used in this analysis was deposited on 16-Jan-06 (Table 1). SNOSS was initialized using measured weak layer density from the first measurement interval. Hourly precipitation measurements were obtained from the adjacent precipitation gauge. For a complete review of the operation of SNOSS, see Conway and Wilbour (1999).

Figure 4 illustrates the modeled output from SNOSS using observations from the Mt Fidelity study plot in the Columbia Mountains. Initial snow density was 56 kg m^{-3} and initial snow temperature was - 9.7 °C. Over the time series SNOSS over-predicted weak layer density at the

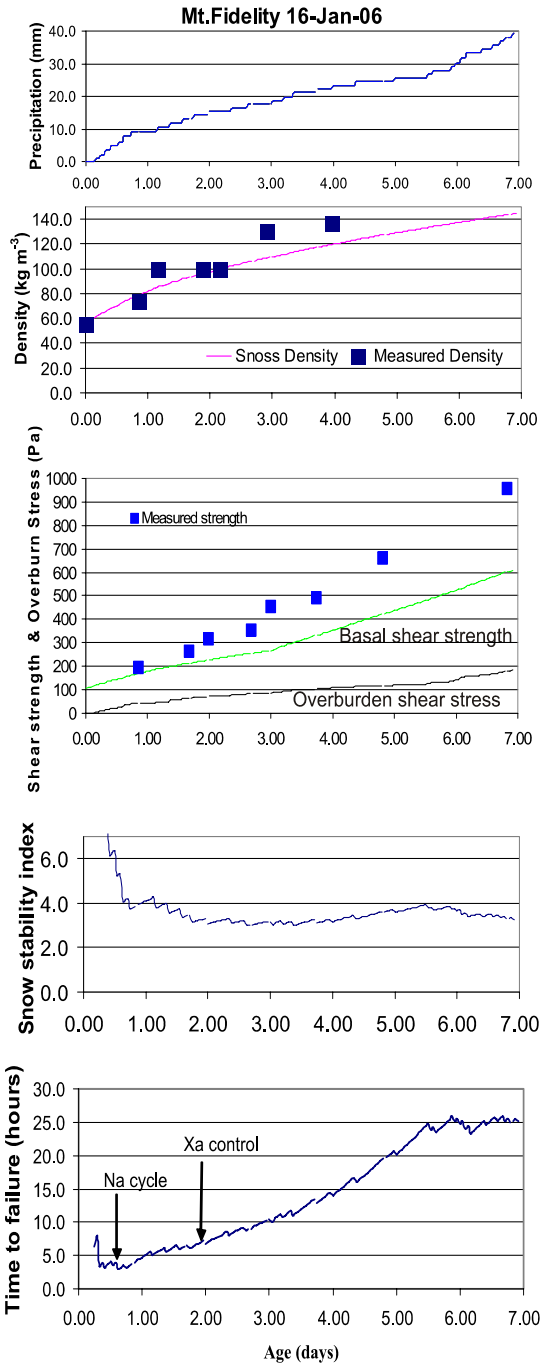

Figure 4. SNOSS outputs for weak layer 16-Jan-06.

beginning of the interval and unpredicted density after day 3 (Figure 4). SNOSS modeled lower shear strengths then measured over the entire time series, with greater deviation in values with increasing age. The results do show a rapidly dropping stability index and a low time to failure when natural avalanche activity was observed (Figure 4). Jamieson et al. (2006) suggest that critical values of stability indices are shown to be less useful than their trends for forecasting natural dry slab avalanches. Often a rapid decrease in the stability index indicates the timing of an avalanche cycle. One cause decreasing stability indices is a large increase in overburn load over a short time period; such is the case during periods of strong precipitation and high winds.

6. CONCLUSIONS

Storm snow weak layers can act as a failure plane for natural slab avalanches. Information about the strength of these layers can aid in forecasting the timing of avalanching. The model developed in this study uses a number of predictor variables to estimate shear strength. These include, age, slab thickness, slab density, and temperature 5 cm below the weak layer.

The model explains 82% of the variability in the initial estimation of shear strength, and between 88% and 83% of the variability in the data for forecasted shear strength using the two model variations. The daily automatic and daily manual models presented are accurate to within 26% and 29% respectively, of measured 'End' of interval shear strength.

In order to determine if the presented shear strength model can be used in snow climates outside of the Columbia mountains, time series observations of storm snow weak layers in other regions are required.

7. ACKNOWLEDGEMENTS

We thank Laura Bakermans, James Floyer, Dave Gauthier, Cam Campbell, Ali Haeri, Paul Langevin, and Ken Matheson for snowpack observations. Special thanks to the Avalanche Control Section at Glacier National Park and Mike Wiegele Helicopter Skiing for logistical support and access to operational study plots. This project could not have been completed without their support.

For support, we are grateful to the Natural Sciences and Engineering Research Council of Canada, Helicat Canada, Canadian Avalanche Association, Mike Wiegele Helicopter Skiing, Canada West Ski Area Association, and Parks Canada.

8. REFERENCES

Brown, C., and Jamieson, B., 2006. Evolving shear strength, stability and snowpack properties in storm snow. In: J.A. Gleason (editor), Proceedings of the 2006 International Snow Science Workshop in Telluride, CO., pp. 15-21.

Brown, R.L., Satyawali, P., Lehning, M., and Bartlet, P., 2001. Modeling the changes in microstructure of snow during metamorphism. *Cold Regions Science and Technology* 33, 91-101.

Canadian Avalanche Association (CAA), 2007. Observation guidelines and recording standards for weather, snowpack, and avalanches. CAA, Revelstoke, BC.

Chalmers, T., 2001. Forecasting shear strength and skier-triggered avalanches for buried surface hoar layers. MSc Thesis, Dept. of Civil Engineering, University of Calgary, Calgary, Alberta, Canada, 109pp.

Colbeck, S.C. 1987. A review of the metamorphism and classification of the seasonal snow cover. Avalanche Formation, Movement and Effects, B. Salm and H. Gubler, ed. International Association of Hydrological Sciences, Publication No. 162, 3-33.

Conway, H. and J. Abrahamson, 1988. Snow-slope stability - A probabilistic approach, Journal of Glaciology, 34, 170-177.

Conway, H. and C. Wilbour. 1998. Why measure new snow density, precipitation and air temperature? Proceedings of the 1998 International Snow Science Workshop in Sunriver, Oregon. Stevens Pass Ski Area, P.O. Box 98, Skykomish, WA, 466-473.

Conway, H., and Wilbour, C., 1999. Evolution of snow slope stability during storms. Cold Regions Science and Technology, 30, 67–77.

Föhn, P., 1987. The stability index and various triggering mechanisms. In: Salm, B., Gubler, H. (Eds.), Avalanche Formation, Movement and Effects, International Association of Hydrological Sciences, Publication, vol. 162, pp. 195-211.

Green, E., Birkeland, K., Elder, K., Johnson, G., Landry, C., McCammon, I., Moore, M., Sharaf, D., Sterbenze, C., Tremper, B., and Williams, K., 2004. Snow, weather, and avalanches: Observational guidelines for avalanche programs in the United States. American Avalanche Association, Pagosa Springs, Colorado, 140 pp.

Gubler, H. 1982. Strength of bonds between ice grains after short contact times. *Journal of Glaciology* 28(100), 457-473.

Hayes, P., C. Wilbour, R. Gibson, H.P. Marshall and H. Conway. 2005. A simple model of snow slope stability during storms. ISSW 2004 Proceedings – A merging of theory and practice, International Snow Science Workshop, 19-24 September 2004, Jackson Hole, Wyoming. USDA Rocky Mountain Research Station, Fort Collins, Colorado.

Jamieson, J.B., 1995. Avalanche prediction for persistent snow slabs. Ph.D. Thesis, Dept. of Civil Engineering, University of Calgary, Canada.

Jamieson, J.B., Johnston, C.D., 1993. Shear frame stability parameters for large scale avalanche forecasting. Annals of Glaciology, 18, 268–273.

Jamieson, B., and Johnston, C., 1999. Snowpack factors associated with strength change of buried surface hoar layers. Cold Regions Science and Technology, 30, 19-34.

Jamieson, B., A. Zeidler and C. Brown. 2007. Explanation and limitations of study plot stability indices for forecasting dry snow slab avalanches in surrounding terrain. *Cold Regions Science and Technology*: 50(1-3), 23-34, doi: 10.1016/j.coldregions.2007.02.010.

Johnson, G., 2000. Observation of Faceted Crystals in Alpine Snowpacks. MSc Thesis. Dept. of Civil Engineering, University of Calgary, Calgary, Alberta, Canada, 98 pp.

Kojima, K., 1967. Densification of seasonal snow cover. In: Oura H. (ed.) Physics of Snow and Ice Vol. I Part 2, Proceedings of a Conference on Physics of Snow and Ice, Institute of Low Temperature Science, Hokkaido University. 929-952.

Schleiss, V., 1989. Rogers pass Snow Avalanche Atlas, Glacier National Park, British Columbia, Canada. Parks Canada, Revelstoke, BC.

Schleiss, V.G., Schleiss, W.E., 1970. Avalanche hazard evaluation and forecast, Rogers Pass, Glacier National Park. Ice Engineering and Avalanche Hazard Forecasting and Control, National Research Council of Canada, Technical Memorandum, vol. 98, pp. 115–121.

Schweizer, J., Föhn, P., 1996. Avalanche forecasting—an expert system approach. Journal of Glaciology, 42, 318–332.

Sommerfeld, R., 1980. Statistical models of snow strength. Journal of Glaciology, 26, 217-223.

Sommerfeld, R., 1984. Instructions for using the 250 cm^2 shear frame to evaluate the strength of a buried snow surface. USDA Forest Service Research Note RM-446, pp.1-6.

Szabo, D., and Schneebeli, M., 2006. Sub-second sintering of ice. Geophysics Research Abstracts, 8, 06327.

Wilks, D., 1995. *Statistical Methods in the Atmospheric Sciences,* Academic Press, 467pp.

Zeidler, A., 2004. Forecasting skier-triggered avalanches in the Columbia Mountains of Canada. PhD thesis. Dept. of Civil Engineering, University of Calgary, Calgary, Alberta, Canada, 264pp.